MAJOR ARTICLE

Small Molecule Targeting Malaria Merozoite Surface Protein-1 (MSP-1) Prevents Host Invasion of Divergent Plasmodial Species

Rajesh Chandramohanadas,[1,2] Basappa,[1] Bruce Russell,[3] Kingsley Liew,[1] Yin Hoe Yau,[4] Alvin Chong,[1] Min Liu,[1] Karthigayan Gunalan,[4] Rahul Raman,[5] Laurent Renia,[6] Francois Nosten,[7,8] Susana Geifman Shochat,[4] Ming Dao,[1,9,a] Ram Sasisekharan,[1,5] Subra Suresh,[10] and Peter Preiser[1,4,a]

[1]Interdisciplinary Research Group of Infectious Diseases, Singapore MIT Alliance for Research and Technology Centre (SMART), [2]Singapore University of Technology and Design, 20 Dover Drive, [3]Department of Microbiology, Yong Loo Lin School of Medicine, National University of Singapore, and [4]School of Biological Sciences, Nanyang Technological University, Singapore; [5]Department of Biological Engineering, Massachusetts Institute of Technology, Cambridge, Massachusetts; [6]Singapore Immunology Network (SIgN), Agency for Science, Technology and Research (A*STAR); [7]Shoklo Malaria Research Unit, Mae Sot, Thailand; [8]Centre for Tropical Medicine, Nuffield Department of Clinical Medicine, Oxford University, United Kingdom; [9]Department of Materials Science and Engineering, Massachusetts Institute of Technology, Cambridge; and [10]Department of Biomedical Engineering and Department of Materials Science and Engineering, Carnegie Mellon University, Pittsburgh

Malaria causes nearly 1 million deaths annually. Recent emergence of multidrug resistance highlights the need to develop novel therapeutic interventions against human malaria. Given the involvement of sugar binding plasmodial proteins in host invasion, we set out to identify such proteins as targets of small glycans. Combining multidisciplinary approaches, we report the discovery of a small molecule inhibitor, NIC, capable of inhibiting host invasion through interacting with a major invasion-related protein, merozoite surface protein-1 (MSP-1). This interaction was validated through computational, biochemical, and biophysical tools. Importantly, treatment with NIC prevented host invasion by *Plasmodium falciparum* and *Plasmodium vivax*—major causative organisms of human malaria. MSP-1, an indispensable antigen critical for invasion and suitably localized in abundance on the merozoite surface represents an ideal target for antimalarial development. The ability to target merozoite invasion proteins with specific small inhibitors opens up a new avenue to target this important pathogen.

Keywords. malaria; *Plasmodium falciparum*; *Plasmodium vivax*; glycan mimetic small molecules; chemical biology; mass spectrometry; red blood cell; host invasion; merozoite surface proteins.

Malaria remains a major health concern for the developing world. Although recent trends suggest a progressive decline, nearly 220 million malaria infections (causing approximately 700 000 deaths) occurred in 2010 alone (http://www.who.int/malaria/world_malaria_report_2011/en/). These data largely focus on *Plasmodium falciparum* infections in Africa and gravely underestimate the contribution of *Plasmodium vivax*, which may account for another 200 million infections in Asia and South America. Thus, malaria against which vaccine development efforts are still ongoing [1] exerts an enormous burden on global human health [2]. Efforts to treat malaria largely rely on chemotherapeutic approaches to block parasitic replication besides preventive measures targeting the mosquito vector. However, recent emergence of resistance against chloroquine [3] and reduced efficacy of artemisinin [4] point to the critical need for exploring new set of antimalarial targets.

Merozoite entry into erythrocytes is driven by complex recognition events between parasitic proteins and sugar moieties on the host red blood cells (RBCs) [5, 6]. Merozoites bind to sialic acid residues on RBC receptors for invasion [7], however, sialic acid-independent invasion pathways have also been elucidated [8, 9].

Received 16 January 2014; accepted 5 May 2014; electronically published 26 May 2014.

Presented in part: Molecular Approaches to Malaria (MAM) 2012, Lorne, Australia,19–23 February 2012; ASTMH 62nd Annual Meeting, Marriott Wardman Park Washington, DC, 13–17 November 2013

[a]P. P. and M. D. contributed contributed equally to this work and are both corresponding authors.

Correspondence: Peter Rainer Preiser, PhD, School of Biological Sciences, Nanyang Technological University, 60 Nanyang Drive Singapore 637551, Republic of Singapore (prpreiser@ntu.edu.sg).

The Journal of Infectious Diseases® 2014;210:1616–26

DOI: 10.1093/infdis/jiu296

Although several plasmodial proteins play critical roles during invasion, merozoite surface proteins (MSPs) and apical membrane antigens (AMAs) have been the most studied. Among MSPs, MSP-1 is considered a prime candidate for vaccine development [10, 11]. It is required for the attachment of merozoites to host receptors such as Band 3 [12] and for normal parasitic development [13]. MSP-1 undergoes 2 proteolytic processing steps during merozoite maturation [14]. Following cleavage, MSP-1 complex remains noncovalently attached to the merozoite surface until invasion, except for a small fragment of 19-kDa from the C-terminus (MSP-1_{19}) that remains attached to the merozoite even after invasion. Antibodies targeting MSP-1_{19} epitopes [15, 16] block merozoite invasion, illustrating a definite invasion-associated role of this domain. In addition, MSP-1_{19} is involved in normal parasitic development [16] and food vacuole formation [17].

Glycan derivatives interfere with replication and invasion of *P. falciparum* [18–20]. Especially, sulfated glycosaminoglycans are known to block merozoite [21] and sporozoite invasion [22]. It has been shown that heparin blocks merozoite invasion by binding to a specific domain of MSP-1 termed MSP-1_{33} thereby preventing the secondary proteolytic processing [23]. Although MSP-1_{19} does not bind to heparin-like glycosaminoglycan oligosaccharides [23], its ability to bind to small molecules has not been investigated. In this study, we report the identification of a small molecule, 2-butyl-5-chloro-3-(4-nitro-benzyl)-3H-imidazole-4-carbaldehyde (NIC) capable of binding to MSP-1_{19} of human malaria parasites: *P. falciparum* and *P. vivax*. Using different approaches, we demonstrate that NIC interacts with EGF-like domains present on MSP-1_{19}. These observations collectively point to the possibility of targeting plasmodial invasion proteins for antimalarial drug development.

MATERIALS AND METHODS

Parasites and Reagents

Collection of blood for *Plasmodium* culture was verified and approved by the Institutional Review Board (IRB) of National University of Singapore (NUS). *P. falciparum* strain 3D7 was used for all experiments unless otherwise stated. Transgenic parasites - D10-*Pf*M3′ and D10-*Pc*MEGF [24] were gifted by Paul Gilson and Danny Wilson (Burnet Institute, Australia). Various recombinant MSP-1_{19} (MRA 47, MRA 48, MRA 55, and MRA 60), antibodies (MRA 3, MRA 16), and parasites (Dd2, K1, T9-94, W2-mef, and FCR3) were obtained from Malaria Research and Reference Reagent Resource Center (MR4). Parasites were synchronized by sorbitol selection or MACS separation (Miltenyi Biotec). Parasitemia was scored by flow cytometric counting (LSRII flow cytometer- BD Biosciences) after staining with Hoechst. Dose-response curve generation and half maximal inhibitory concentration (IC50) determination were performed with GraphPad Prism 5 using a four-parameter logistic curve (variable slope).

Virtual Screening and Design of Novel MSP-1 Ligands

Insight II (Accelrys) was used for molecular modeling [25]. Automatic docking, clustering and energy minimizations [26] were performed using LigandFit module. A cavity detection algorithm and Monte Carlo conformational search algorithm were used for generating ligand poses consistent with active site shapes. Ligand poses at these sites were selected based on shape matching, using a cutoff distance of 3 Å. Structure based high-throughput virtual screening method of LigandFit (DS version 2.5) was used to identify potential ligands that interact with MSP-1 (PDB ID: 1CEJ) using NCBI database [27]. Glycan-mimetic small molecules such as **KI-105**, **DMBO**, **BIC**, **NIC**, **CIC**, and **DIC** were synthesized as reported [28]. These compounds were purified and characterized using Agilent 1200 series LC system (Agilent ZORBAX, Eclipse-XDB-C18, 5 µm, 4.6 mm × 150 mm).

Docking of Small Molecule Ligands to MSP-1_{19}

All ligands were subjected to LigandFit docking to determine reasonable conformations for each low energy conformer at the binding site. Initially, crystal structures of MSP-1_{19} from *P. falciparum* [29] (PDB ID: 1CEJ), *P. vivax* [30] (PDB ID: 2NPR) and *P. knowlesi* [31] (PDB ID: 1N1I) were used for docking. Further, homology modeling of the MSP-1_{19} domains for *P. chabaudi*, *P. malariae*, and *P. ovale* were performed using 'build homology modeling' protocol by DS version 2.5.

SPR Measurements

SPR measurements were conducted using a Biacore T-200 instrument (Biacore, GE Healthcare). MSP-1_{19} peptide was directly immobilized onto a flow cell on a CM5-S sensor chip (Biacore, GE Healthcare) through standard amine coupling [32]. An empty flow cell was used as control. Surface was activated for 7 minutes with 1:1 mixture of 0.2 M N-ethyl-N'-[3-(diethylamino)propyl]carbodiimide (EDC) and 0.05 M N-hydroxysuccinimde (NHS). Different interactants (in 10 mM sodium acetate, pH 4.0) was injected across the activated surface at 10 µL/min until desired immobilization level of approximately 3000 RU was achieved. The surface was blocked with 7-minute injection of 1 M ethanolamine-HCl, pH 8.5. Small molecules were screened against the immobilized protein at a flow rate of 30 µL/min, with a 60-second association phase and a 5-minute dissociation phase, in running buffer (20 mM Na_2HPO_4-NaH_2PO_4, pH 7.4, 150 mM NaCl, 5% DMSO). Measurements for affinity determination were performed under similar conditions using 2-fold dilutions of 10 µM. Sensorgrams were double referenced [33] and evaluated with Scrubber 2 software. Equilibrium responses against concentration were fitted to a simple 1:1 binding isotherm using a global R_{max}. Each experiment was

Table 1. Summary of Docking and Scoring Analyses Among the Selected Small Molecule Scaffolds Against *Pf*MSP-1_{19}

Ligand	MW	PLP1	PLP2	LigScore1	LigScore2	Jain	PMF	LIE	Dock Score
NIC	321.7	82.9	65.0	2.6	1.2	−0.3	36.0	1.4	45.0
CIC	339.2	46.4	46.7	1.9	3.2	0.6	27.1	−3.4	33.5
BIC	415.7	58.0	43.1	1.3	4.1	−1.9	55.9	−1.3	37.6
DIC	283.7	66.5	71.6	2.4	3.2	3.3	−18.0	–	27.6
KI-105	379.3	55.6	42.3	1.1	3.9	2.4	44.6	−2.1	38.6
DMBO	373.4	. . .	. . .	. . .	. . .	. . .	. . .	. . .	. . .

Abbreviations: DS, dock score; Jain, empirical scoring function through an evaluation of the structures and binding affinities of a series of protein-ligand complexes; LIE, ligand internal energy; PLP1, piecewise linear potential 1; PLP2, piecewise linear potential 2; PMF, potential of mean force.

carried out at least 3 times. To validate the selectivity of binding and to approximately estimate the affinity constants, simulation exercise were carried out as reported [34].

Localization and Affinity-enrichment of the Target Using NIC-Biotin

NIC- biotin was synthesized by amine coupling of the aldehyde group. Late-stage schizonts (approximately 45 hpi) were treated with NIC-biotin for 4 hours, and aliquots were fixed (0.1% paraformaldehyde/phosphate-buffered saline [PBS]) and permeabilized (0.2% Triton X100/PBS) in presence of Casein. After washing, samples were incubated with phycoerythrin-conjugated streptavidin (Invitrogen) and Hoechst for 30 minutes. Fluorescence microscopy was performed using an LSM 710 confocal microscope (Carl Zeiss). For affinity purifying NIC-reactive proteins, schizonts (approximately 48 hpi) were fractionated into extraparasitic and parasitic fractions by extraction with 0.02% saponin and 1% Triton X-100 sequentially. Samples were then diluted 1:5 with 20 mM sodium acetate buffer (pH 5.5), treated with 50 μM NIC-biotin for 2 hours, and incubated with streptavidin-agarose beads (Thermo Scientific). After removing unbound proteins by centrifugation, pellet was washed with PBS and proteins extracted for SDS-PAGE. Coomassie staining was carried out to visualize polypeptides. Protein bands were excised and subjected to MALDI/TOF-TOF analyses (4800 Proteomics Analyser- Applied Biosystems). MS data were searched using MASCOT v 2.1 (Matrix Science Ltd, London, UK) against NCBI Database. For examining target-specificity, affinity enrichment experiments were performed with (1) nonbiotinylated NIC, (2) in competition with excess of NIC (100 μM), and (3) denatured (SDS/heat) sample. Proteins bound to streptavidin beads were collected, resolved on SDS-PAGE for Western blotting using anti-MSP-1 antibody.

Plasmodium vivax Ex Vivo Invasion Assays

During February 2012, samples from *P. vivax* infected patients at Shoklo Malaria Research Unit (SMRU), Mae Sot region (Thailand) were collected after written informed consent. Cord blood was taken from 3 post healthy delivery placentas. The samples were collected as per ethical guidelines in the approved protocols: OXTREC 027-025 (University of Oxford, Centre for Clinical Vaccinology and Tropical Medicine, UK) and MUTM 2008-215 from the Ethics Committee of the Faculty of Tropical Medicine, Mahidol University, Bangkok. Leukocytes and platelets were removed using a CF11 column ([35]) before conducting *P. vivax* invasion assays as described elsewhere [36]. An inert chemical intermediate of the synthetic scheme, 2-butyl-5-chloro-4-carbaldehyde (BCI) at a concentration of 200 μM and 25 μg/mL of anti-Duffy receptor DARC antibody (gift by Drs Colin and Bertrand; Institut National de la Transfusion Sanguine, 75015 Paris, France) served as negative and positive controls respectively. To determine invasion rates, a 3 color cytometery method [37] using a field flow cytometer (BD Accuri C6) was used. Flow cytometery data was verified with Giemsa-stained smears using microscopy.

RESULTS

Identification of NIC as a Potential Ligand Against EGF-like Domains of Plasmodial MSP-1

Antibodies targeting EGF-like domains on the C-terminal motif (MSP-1_{19}) prevent host invasion. We therefore set out to identify small molecules that can bind to MSP-1_{19} domain as invasion blockers. First, using the solution structure [29] a virtual screening was performed to prioritize small molecules that could interact with MSP-1_{19} of *P. falciparum*. Based on this screening, we chose KI-105 [38] and DMBO [39] that are known to interact with EGF-like domain containing proteins in other systems as promising ligands to interact with MSP-1_{19}. However, neither KI-105 nor DMBO exhibited any antimalarial activity against *P. falciparum*. Thus, we synthesized and evaluated other related scaffolds such as BIC, NIC, CIC, and DIC (Supplementary Figure 1*A*) as binders of MSP-1_{19}. Among these, it was earlier demonstrated that NIC binds to vascular endothelial growth factor (VEGF) resulting in reduced cancer cell proliferation [40].

Based on these computational analyses, we posited that NIC could bind with a higher affinity to EGF-like domains present on MSP-1_{19} compared to other structurally related

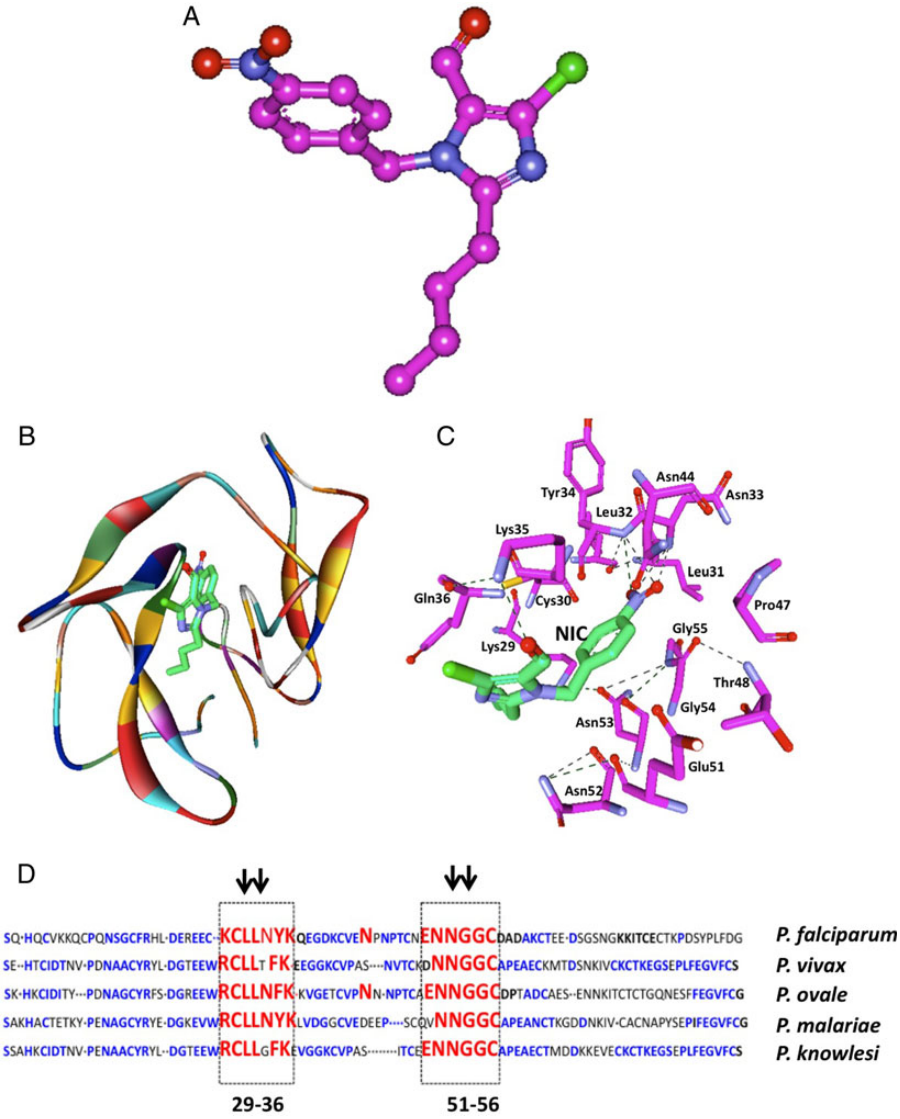

Figure 1. Prediction of NIC as a small molecule scaffold with potential binding affinity to MSP-1_{19} of *Plasmodium falciparum*. *A*, energy minimized structure of NIC highlighting its ionic functional groups (highlighted with arrowheads) is shown. *B*, Ribbon diagram of the structure of EGF-like domain of *Pf*MSP-1_{19} in complex with NIC is shown. Secondary structure of the protein is shown with α-helices and β-strands, whereas NIC is represented in ball-and-stick model (green for carbon, blue for oxygen, white for hydrogen, and yellow for sulphur). *C*, Interaction map showing the key amino acids at *Pf*MSP-1_{19} that are positioned to make interactions with NIC. The hydrogen bonding is shown in red. *D*, Sequence alignment of C-terminal residues of MSP-1_{19} of various plasmodial species: conserved amino acid residues are in blue, residues that are likely to interact with NIC are highlighted in red. Abbreviation: NIC, 2-butyl-5-chloro-3-(4-nitro-benzyl)-3H-imidazole-4-carbaldehyde.

compounds (Table 1). The energy-minimized structure of NIC is highlighted in Figure 1*A*. The ribbon diagram showing the structure of EGF-like domain of *Pf*MSP-1_{19} in complex with NIC is shown as a ball-and-stick model (Figure 1*B*). Based on the structural complex of NIC with *Pf*MSP-1_{19}, the key residues positioned to make contact with NIC included Lys29, Cys30, Leu31, Leu32, Asn33, Tyr34, Lys35, and Gln36. NIC was likely to form additional bonds with Glu51, Asn52, Asn53, Gly54 and Gly55 (Figure 1*C*). Also, it appears that NIC has the unique ability to bind to MSP-1_{19} through its ionic nitro-group on the benzene ring making it the most suitable ligand. Sequence alignment of residues within the EGF-like domains of MSP-1_{19} from multiple plasmodia revealed remarkable conservation of key residues that are positioned to make contact with NIC (Figure 1*D*). Many of these conserved residues were within epitopes recognized by invasion-blocking antibodies against MSP-1.

NIC Specifically Interacts with *Pf*MSP-1_{19}

Computational analyses predicted that among KI-105 variants (BIC, NIC, CIC, and DIC), NIC had the highest binding affinity to MSP-1_{19}. This was validated via surface plasmon resonance (SPR) measurements using recombinant *Pf*MSP-1_{19}, where

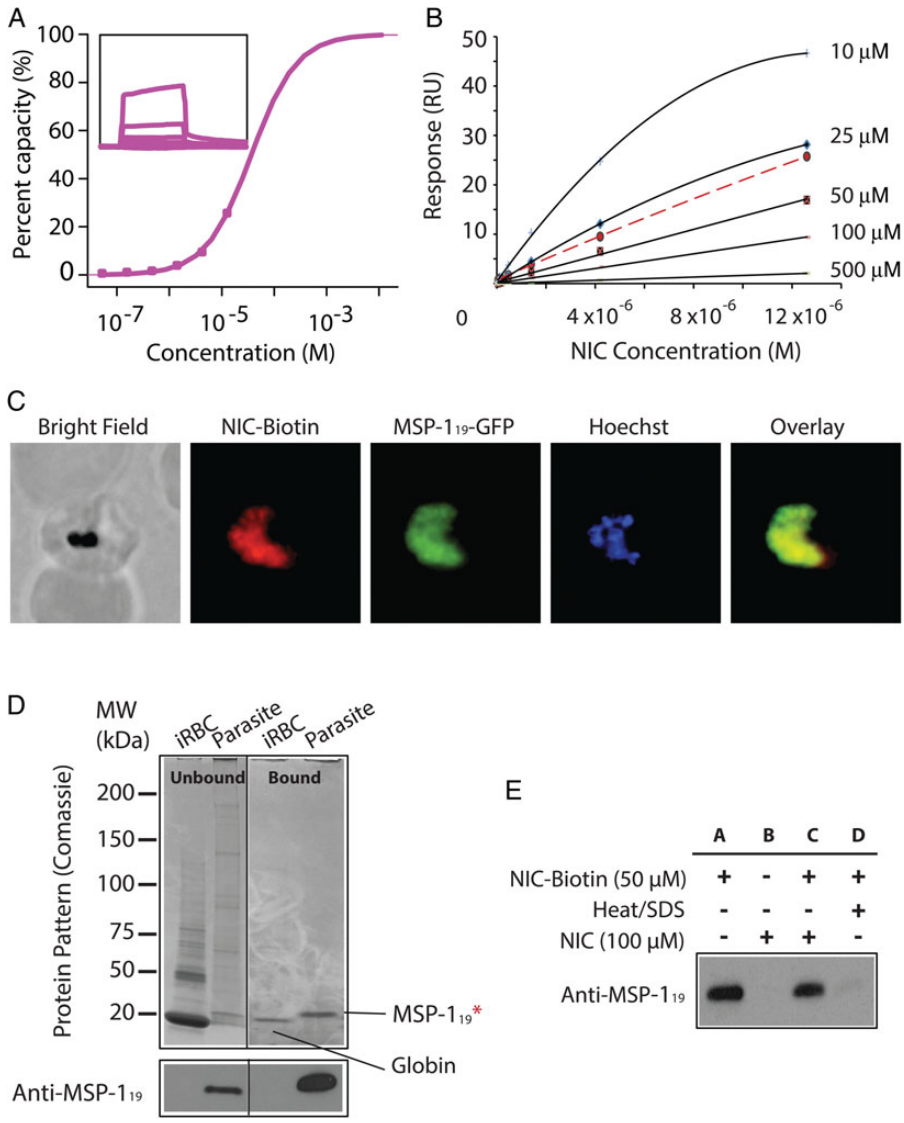

Figure 2. NIC interacts specifically with MSP-1_{19} of *Plasmodium falciparum*. *A*, SPR Interaction analysis of NIC over immobilized *Pf*MSP-1_{19}. Immobilization was performed by amine coupling to a CM5 sensor chip to the level of 3000 RU. NIC (concentrations) was injected sequentially over the relevant and control surfaces. The sensorgrams were fit using the steady state affinity model from Scrubber software. Each experiment was carried out at least 3 times to confirm the results. *B*, Experimental values of Req for the corrected sensorgrams were compared to the simulated values for K_D = 10 μM and 50 μM. The value for the affinity constant cannot be determined from equilibrium analysis (see results) and was estimated to be between these 2 values (37 μM as calculated from the fit). *C*, Fluorescent microscopy analyses using NIC-biotin reveals the target on merozoite surface, co-localizing with MSP-1_{19}-GFP. *D*, Affinity purification of proteins using 50 μM NIC-biotin shows specific enrichment of MSP-1_{19}. Magnet purified parasites were fractionated into extraparasitic and merozoite fractions and incubated with NIC-biotin. SDS-PAGE analysis of biotinylated proteins showed specific enrichment of a polypeptide later confirmed to be MSP-1_{19} by mass spectrometry analysis and Western blot. *E*, Affinity pull-out experiments of parasitic material using 50 μM NIC-biotin (lane A), 50 μM NIC (lane B), 100 μM NIC followed by 50 μM NIC-biotin (lane C), and under denaturing conditions (lane D). The latter 3 conditions significantly reduced the extent of *Pf*MSP-1_{19} enrichment. Abbreviation: NIC, 2-butyl-5-chloro-3-(4-nitro-benzyl)-3H-imidazole-4-carbaldehyde.

none of the small molecules showed detectable binding to *Pf*MSP-1_{19} except NIC (Figure 2*A*). Notably, BCI, which served as the negative control as well as heparin, showed no measurable interaction with MSP-1_{19} as expected from previous reports [23].

We determined the affinity constant from a fit to a simple binding isotherm in an equilibrium analysis, with an estimated value in the tens of micromolar range (approximately 37 μM; Figure 2*B*). Because we could not reach saturation of the surface due to lack of solubility of NIC at high concentrations (under conditions used for SPR measurements), and thus the calculated value of Rmax could not be precise, we chose to show the range for the value of affinity constant by simulating the Req values vs the NIC concentration for affinities of 25 and 50 μM and plotting the experimental values for Req at different

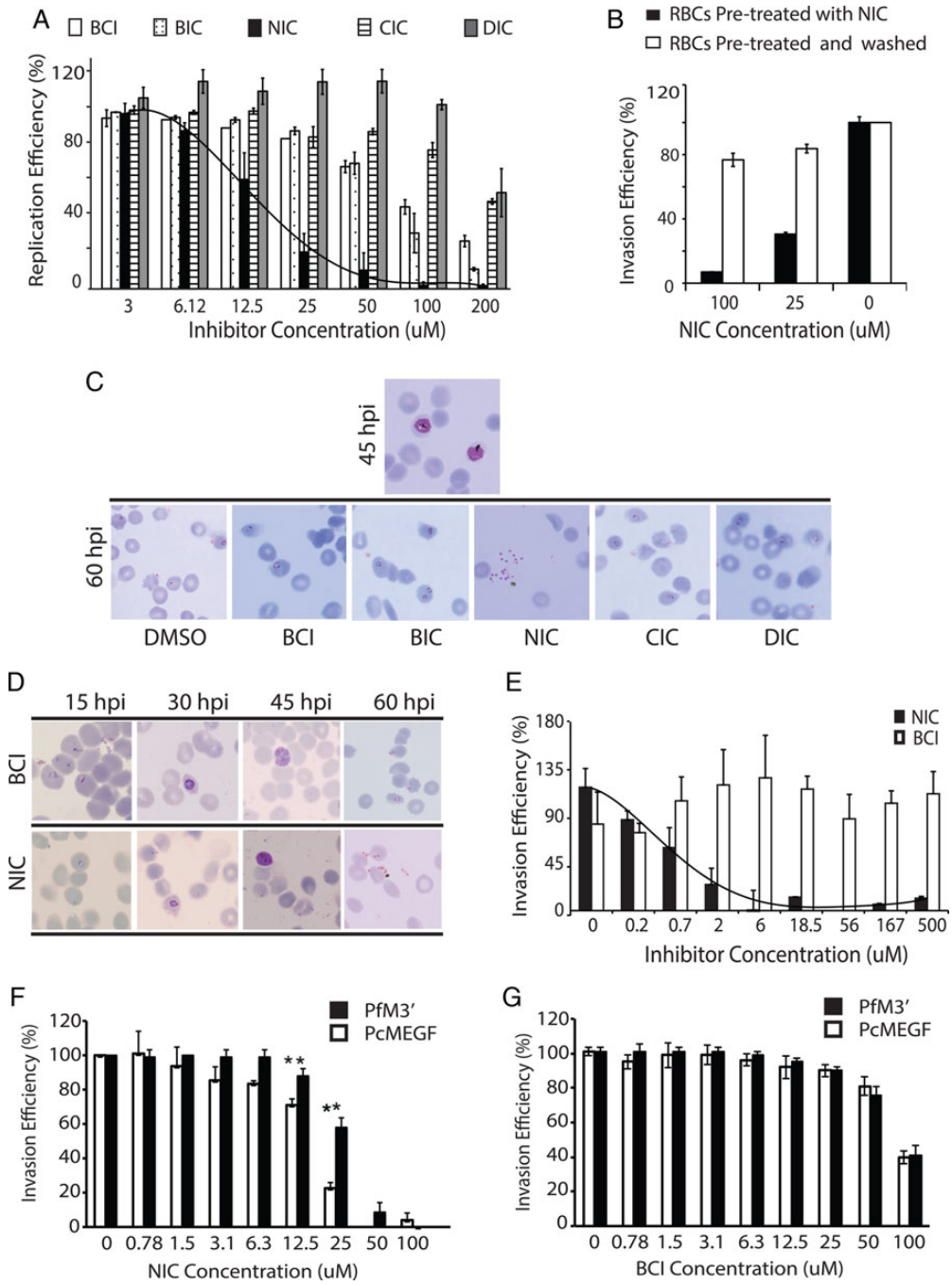

Figure 3. Evaluation of invasion-blocking properties of NIC in *Plasmodium falciparum*. *A*, Dose-dependent effect of 4 major small molecule scaffolds on the replication of *P. falciparum*; NIC shows a significant and specific inhibition of parasite replication (transition from schizonts to ring) with an average IC50 of 21.7 μM, error bars show standard deviation, the figure represents compiled data from 3 independent experiments. *B*,RBCs preincubated with NIC and washed prior to parasite infection, supports normal invasion and growth ruling out nonspecific binding of NIC to red cell proteins. *C*, Microscopic analysis of representative Giemsa-stained smears from inhibitor-treated parasites (DMSO, BCI, BIC, NIC, DIC, and CIC each at 25 μM) demonstrate that treatment with NIC resulted in an invasion defective phenotype, clumps of extracellular merozoites that were unable to invade was observed. None of the other inhibitors induced similar phenotypes at the tested concentration. *D*, Stage-specific effect of NIC (25 μM) on *P. falciparum* development demonstrating a specific inhibitory effect on invasion. *E*, The inhibitory effect of NIC on red cell invasion by purified merozoites, the figure shows combined data from 4 independent experiments and error bars indicate standard deviation. *F*, Transgenic parasites (*Pc*MEGF) that contain MSP-1_{19} from *Plasmodium chabaudi* (*Pc*MSP-1_{19}) at schizont stages were allowed to rupture and invade in presence of NIC**.** These parasites showed increased sensitivity to NIC compared to wild-type (*Pf*M3′) parasites. The figure represent combined results from 3 independent experiments, error bars show standard deviation. *G*, Transgenic parasites (*Pc*MEGF) that contain MSP-1_{19} from *Plasmodium chabaudi* (*Pc*MSP-1_{19}) when allowed to rupture and invade in presence of BCI, showed no differences in their sensitivity. The figure represents combined results from 3 independent experiments; error bars show standard deviation. Abbreviation: NIC, 2-butyl-5-chloro-3-(4-nitro-benzyl)-3H-imidazole-4-carbaldehyde.

concentrations of NIC, as adopted elsewhere [34]. Figure 2*B* shows that the values of responses for the measured interaction between NIC and *Pf*MSP-1_{19} do fall between 25 and 50 μM.

To validate the interaction of NIC with its parasitic target, we first conducted co-localization experiments using NIC-biotin (Supplementary Figure 1*B* and 1*C*) that has comparable invasion inhibitory effects on malaria parasites as NIC (Supplementary Figure 1*D*). Using a parasite line that expresses MSP-1_{19}-GFP, we observed co-localization of NIC-biotin with MSP-1 in late-stage schizonts (Figure 2*C*). In contrast, ring or trophozoite stage parasites when very little MSP-1 is present showed no detectable labeling with NIC-biotin (Supplementary Figure 1*E*). However, due to the dispersed nature of GFP distribution in these parasites [41], it was not possible to conclusively document co-localization. Hence, fluorescence microscopy was repeated using antibodies against MSP-1_{19} together with NIC-biotin (Supplementary Figure 1*F*); further supporting an interaction between NIC and MSP-1_{19}.

Next, we used NIC-biotin to identify parasitic targets. Schizont-stage parasites were fractionated into infected red cell/extraparasitic (iRBC) and parasitic fractions by differential extraction using saponin [42]. Further, each sample was incubated with 50 μM NIC-biotin and then with streptavidin-agarose beads to affinity purify proteins that interact with NIC. Aliquots from unbound and bound fractions from each sample were resolved on SDS-PAGE and polypeptides visualized by Coomassie staining. Enrichment of a low molecular weight protein (Figure 2*D*) was observed from the parasitic fraction and was identified as MSP-1_{19} through mass spectrometry (Supplementary Figure 1*G*). Importantly, no other proteins, including MSP-1_{33}, the target of heparin as reported previously [23], were enriched in the NIC-bound fraction. Specificity of NIC-biotin binding to MSP-1_{19} was confirmed by conditions such as (*a*) performing affinity-enrichment from parasitic extracts with NIC, (*b*) pretreatment of the extract with 100 μM NIC prior to incubation with NIC-biotin, and (*c*) by performing NIC-biotin incubation after denaturing the sample with SDS/heat (Figure 2*E*). As expected, pretreatment with excess NIC significantly reduced (30%–50%) the affinity enrichment of MSP-1_{19} by NIC-biotin. Due to the multiple steps involved in this experiment where each sample was processed individually, these results are primarily qualitative.

NIC Blocks *P. falciparum* Replication by Impairing Merozoite Invasion

Assays were performed on several *P. falciparum* strains to evaluate the effect of the small molecules on erythrocytic development. Trophozoite-stage parasites (approximately 24 hpi) were allowed to grow until the next cycle in presence of inhibitors. DMSO and BCI served as negative controls; 48 hours later, samples were collected, stained with Hoechst, and parasitemia scored by flow cytometry. Among the scaffolds tested, only

Table 2. Effect of NIC on Various Strains of *Plasmodium falciparum*, Based on Replication Assays (Using Schizont-Stage Parasites)

	IC50 (μM)	
Parasite Strains	BCI	NIC
3D7	>200	21.7 ± 6.2
Dd2	>200	21.0 ± 0.1
FCR3	>200	20.0 ± 0.4
K1	>200	22.5 ± 6.5
T994	>200	23.6 ± 2.4
W2-mef	>200	21.6 ± 8.3
W2-mef (NM)	>200	22.3 ± 6.6

The values represent compiled results from 3 independent experiments.

Abbreviations: BCI, 2-butyl-5-chloro-4-carbaldehyde; IC50, half maximal inhibitory concentration; NIC, 2-butyl-5-chloro-3-(4-nitro-benzyl)-3H-imidazole-4-carbaldehyde.

NIC inhibited parasite replication (Figure 3*A*) with a median IC50 of 21.7 μM. Potential nonspecific interaction of NIC with red cell proteins was ruled out by preincubating RBCs with NIC for 2 hours and washing them prior to mixing with late-stage parasites. RBCs that were pretreated with NIC supported normal parasite invasion and growth (Figure 3*B*). Microscopic evaluation of Giemsa-stained smears revealed that NIC treatment resulted in impaired merozoite invasion. Clumps of agglutinated merozoites were observed in smears prepared from postrupture time points (Figure 3*C*) after NIC treatment. NIC showed comparable inhibitory potential on a number of plasmodial strains tested (Table 2) demonstrating a conserved target.

Further, ring stage parasites (approximately 12 hpi) were treated with 20 μM NIC and phenotypes monitored at specific intervals (15, 30, 45, and 60 hpi) using Giemsa-stained smears. By 60 hpi, all the schizonts had ruptured and established rings in the control (DMSO) treatments, whereas merozoites failed to invade in presence of NIC (Figure 3*D*). The invasion inhibition by NIC was confirmed by live video microscopy [43]. In presence of NIC, the schizonts appeared to burst slowly and despite making initial contact with RBCs, merozoites failed to invade even after several minutes (Supplementary Videos 2*A* and 2*B*). Next, invasion inhibition assays were conducted by mixing purified merozoites [44] with fresh RBCs in presence of NIC. This experiment revealed a strong and specific invasion inhibition in presence of NIC (Figure 3*E*). Negative control (BCI) showed no significant inhibitory effects on invasion even at 200 μM. Although there are minor differences in the sensitivity to the inhibitors of purified merozoites compared to intact schizonts, these experiments provide strong evidence for the invasion inhibitory activity of NIC. Furthermore, schizont-stage parasites (approximately 45 hpi) were exposed for 2 hours to NIC, and NIC was removed by washing. These parasites were

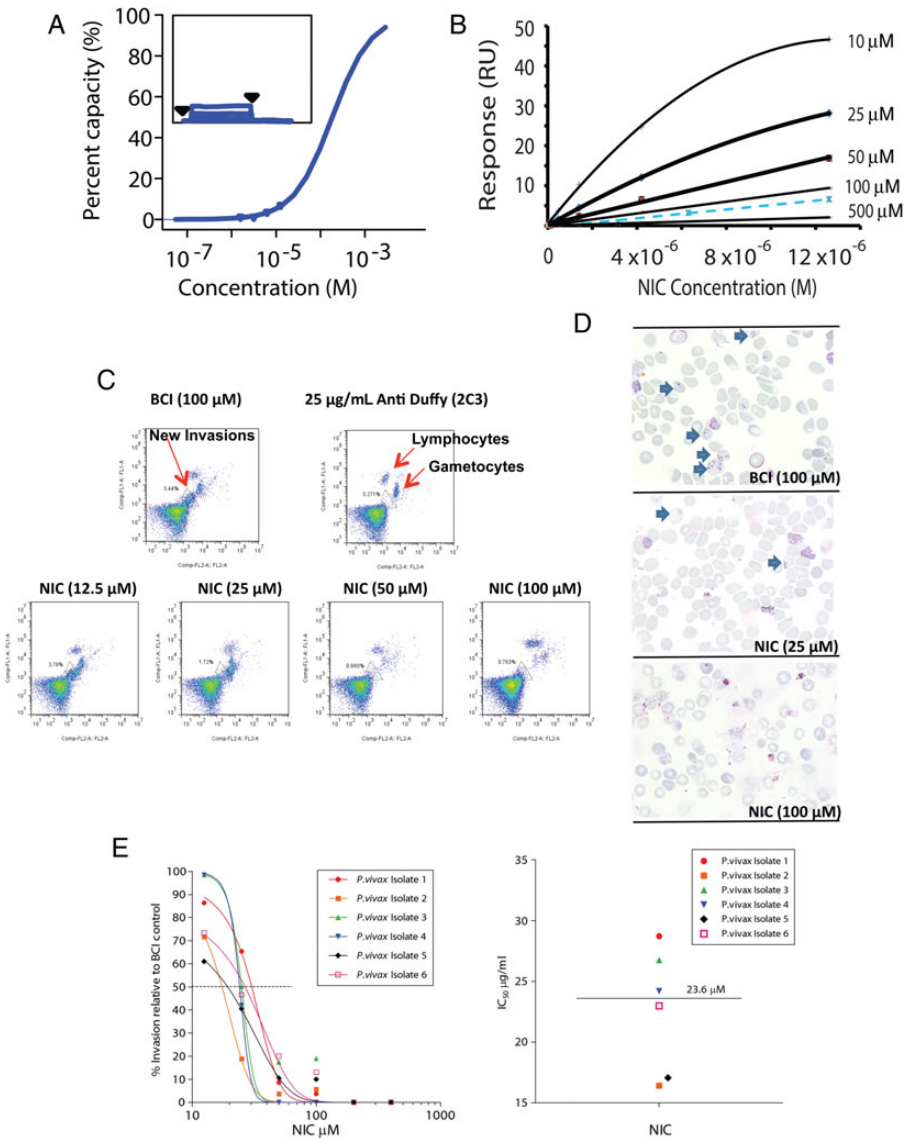

Figure 4. NIC binds to *Pv*MSP-1_{19} and shows anti-invasive activity against clinical isolates of *Plasmodium vivax*. *A*, SPR measurements using recombinant *Pv*MSP-1_{19} reveal specific binding of NIC with the target antigen. Immobilization, the binding assay and the determination of the affinity were performed as in Figure 2. *B*, Experimental values of Req for the corrected sensorgrams were compared to the simulated values for $K_D = 100$ µM and 500 µM. The value for the affinity constant cannot be determined from equilibrium analysis (see results) and was estimated to be between these 2 values. *C*, An ex vivo assay on 6 Thai isolates of *P. vivax* showed that NIC had a dose-dependent inhibitory effect on the invasion of human cord reticulocytes by *P. vivax*, as determined by flow cytometry; BCI as well as an antibody against Duffy protein served as negative and positive controls, respectively. *D*, Microscopic analyses of the Giemsa-stained smears collected from inhibitor-treated cultures reveal blockage of invasion by *P. vivax* in presence of NIC. *E*, Compiled data derived from the treatment with NIC of 6 Thai *P. vivax* isolates analyzed using a nonlinear sigmoidal model provide a median IC50 of 23.6 µM. Abbreviations: IC50, half maximal inhibitory concentration; NIC, 2-butyl-5-chloro-3-(4-nitro-benzyl)-3H-imidazole-4-carbaldehyde.

able to invade efficiently, revealing NIC's specific inhibitory effect solely on invasion (Supplementary Figure 1*H*).

Computational docking revealed that NIC was likely to have superior binding affinity to MSP-1_{19} of *P. chabaudi* (Supplementary 3*A*) compared to *Pf*MSP-1_{19}. Hence, we used a transgenic strain of *P. falciparum* (*Pc*MEGF) that has *Pc*MSP-1_{19} swapped in [24] to evaluate its sensitivity to NIC. Dose-dependent effect of NIC on replication of *Pc*MEGF was examined together with the control parasites (*Pf*M3′) that contain the original *Pf*MSP-1_{19}. This revealed significantly higher sensitivity of the *Pc*MEGF parasites to NIC (Figure 3*F*) compared to *Pf*M3′, in agreement with the computational predictions. BCI-treated parasites (*Pf*M3′ and *Pc*MEGF) served as controls and showed no apparent differences in sensitivity (Figure 3*G*). These data functionally validate the interaction between NIC and MSP-1_{19}, leading to impairment of invasion.

NIC Inhibits *P. vivax* Invasion

The residues within EGF-like domains of MSP-1_{19}, are significantly conserved among multiple plasmodia. Computational analyses predicted that MSP-1_{19} from several human malaria parasites were likely to bind to NIC (Supplementary 3*B*). Hence, we inspected the interaction of NIC with *Pv*MSP-1_{19}, EGF-like domains of which are critical for reticulocyte invasion [45] by *P. vivax*. SPR measurements using recombinant *Pv*MSP-1_{19} confirmed specific interaction of NIC with the target (Figure 4*A*), however with lower affinity compared to *Pf*MSP-1_{19} (Figure 4*B*). The effect of NIC on ex vivo invasion of *P. vivax* into human reticulocytes was tested using a recently developed assay [36]. Purified schizonts from clinical isolates were mixed with enriched reticulocytes in presence of different amounts of NIC. BCI-treated parasites served as negative control while an anti- Duffy antibody (2C3) that blocks invasion at 25 μg/mL concentration served as positive control. After 24 hours, newly invaded reticulocytes were counted by a field-based flow cytometry assay [36] (Figure 4*C*). A concentration-dependent inhibition of invasion by NIC on *P. vivax* merozoites was observed with an average IC 50 of 23.6 μM. BCI showed no inhibition even at 100 μM concentration. These results were further verified by microscopic inspection of Giemsa-stained blood smears (Figure 4*D*). In BCI-treated samples, robust invasion was observed (Figure 4*D*, upper panel), whereas very few ring-stage infections were found in samples that were incubated with 25 or 100 μM NIC (Figure 4*D*, middle and lower panels). Finally, 6 independent analyses were carried out using different field isolates—all of them demonstrated dose-dependent inhibition of invasion caused by NIC (Figure 4*E*), with a Median IC50 of 23.6 μM (IQR 16.9–27.24). These observations are consistent with other results and strongly support the idea that NIC has broad affinity to MSP1_{19} from multiple forms of human malaria.

DISCUSSION

Host invasion by plasmodia is facilitated by coordinated action of merozoite surface proteins [46], proteases [47, 48], and signaling molecules such as calcium [49]. Extracellular merozoites have a short life span; they become nonviable within minutes of release making strategies targeting invasion an attractive proposition. Prior research explored invasion-related proteases [47, 48] as well as antibodies for potential therapeutic development. However, the likely off-target effects of protease inhibitors and permeability limitations of antibodies hinder these approaches significantly.

Chemical biology tools allow detailed and targeted investigation of complex biological events, such as malaria parasite invasion. MSP-1 is the most abundant invasion protein and binds to glycan residues on RBC to initiate host entry. The smaller fragment derived from MSP-1 processing; MSP-1_{19} is critical for invasion and parasite development. It shows less polymorphism (within its EGF-like domains) highlighting suitability as a pan-plasmodial target. We conducted in silico and in vitro screening to identify a small molecule, NIC with significant binding affinity to both recombinant and parasitic *Pf*MSP-1_{19} that inhibits merozoite invasion. Although at this stage we do not fully understand the detailed molecular mechanism leading to invasion inhibition by NIC binding to MSP-1, our results represent a major advancement in the hunt for antimalarials with pan-species efficacy. NIC was able to bind to MSP-1 and inhibit invasion not only upon merozoite release but also within late-stage schizonts. This highlights the permeability advantages of small molecules over therapeutic antibodies. Efforts to optimize molecular structures from the NIC lineage with stronger/irreversible binding properties to MSP-1 may provide a platform to further consider these molecules for in vivo experiments and detailed pharmacological profiling.

The abundance, accessible cellular localization, and indispensable nature of invasion proteins make them promising drug targets. In the *Plasmodial* genome, there are several proteins with putative EGF-like domains. Other members of the MSP family, MSP4 and MSP8 as well as lesser-known proteins such as PF3D7-1403200 and PF3D7-1002300 (www.plasmodb.org) contain such domains. It would be desirable to study these proteins/domains as candidate targets to design small molecule scaffolds, individually or as a "group target." Designing small molecules to target invasion proteins offer a viable option in the development of a resistance-free drug against human malaria.

Supplementary Data

Supplementary materials are available at *The Journal of Infectious Diseases* online (http://jid.oxfordjournals.org). Supplementary materials consist of data provided by the author that are published to benefit the reader. The posted materials are not copyedited. The contents of all supplementary data are the sole responsibility of the authors. Questions or messages regarding errors should be addressed to the author.

Notes

Acknowledgments. The authors thank MR4 for various recombinant proteins and antibodies and Brendon Crabb, Paul Gilson, and Dany Wilson for providing transgenic parasites (D10-*Pf*M3 and D10-*Pc*MEGF). The support from the core facility at the Department of Biological Sciences-NUS in performing mass spectrometry analysis is thankfully acknowledged.

Authors contributions. R. C. designed, performed, and coordinated research, analyzed the data, and wrote the article. B. designed and performed experiments related to chemical synthesis, performed computational analysis and assisted in manuscript writing. B. R. was involved in *P. vivax* study design, performed *P. vivax* invasion assays, analyzed the data, verified results, and assisted in article preparation. K. L. performed *P. falciparum* experiments and assisted in article preparation. Y. H. performed SPR analyses. L. M. assisted with *P. falciparum* experiments. A. C. assisted with *P. falciparum* experiments. K. G. performed microscopy analysis. L. R. was involved in *P. vivax* study design and verified results. F. N. provided reagents and other tools for research, contributed to ethical clearance. S. G. S. was involved in SPR study design, provided research tools, and verified SPR results. R. S. was involved in study design, provided tools for

research, and verified results. M. D. was involved in study design, provided tools for research, and verified results. S. S. was involved in study design, provided tools for research, and verified the results. P. R. P. contributed to study design, provided tools for research, verified the results, and wrote the article.

Financial support. The authors acknowledge Singapore-MIT Alliance for Research and Technology (SMART) Centre funded by The National Research Foundation (NRF) for financial support. R. C. was partially supported by the start-up research grant (SRG LSC 2013 049) from Singapore University of Technology and Design (SUTD). M. D. and S. S. acknowledge partial support from the National Institutes of Health (NIH) grant R01HL094270.

Potential conflicts of interest. All authors: No potential conflicts of interest.

All authors have submitted the ICMJE Form for Disclosure of Potential Conflicts of Interest. Conflicts that the editors consider relevant to the content of the manuscript have been disclosed.

References

1. Agnandji ST, Lell B, Soulanoudjingar SS, et al. First results of phase 3 trial of RTS, S/AS01 malaria vaccine in African children. N Engl J Med **2011**; 365:1863–75.
2. Murray CJ, Rosenfeld LC, Lim SS, et al. Global malaria mortality between 1980 and 2010: a systematic analysis. Lancet **2012**; 379:413–31; doi:10.1016/S0140-6736(12)60034-8.
3. Mita T, Tanabe K, Kita K. Spread and evolution of *Plasmodium falciparum* drug resistance. Parasitol Int **2009**; 58:201–9.
4. O'Brien C, Henrich PP, Passi N, Fidock DA. Recent clinical and molecular insights into emerging artemisinin resistance in *Plasmodium falciparum*. Curr Opin Infect Dis **2011**; 24:570–7.
5. Breuer WV, Kahane I, Baruch D, Ginsburg H, Cabantchik ZI. Role of internal domains of glycophorin in *Plasmodium falciparum* invasion of human erythrocytes. Infect Immun **1983**; 42:133–40.
6. Mayer DC, Cofie J, Jiang L, et al. Glycophorin B is the erythrocyte receptor of *Plasmodium falciparum* erythrocyte-binding ligand, EBL-1. Proc Natl Acad Sci U S A **2009**; 106:5348–52.
7. Sim BK, Chitnis CE, Wasniowska K, Hadley TJ, Miller LH. Receptor and ligand domains for invasion of erythrocytes by *Plasmodium falciparum*. Science **1994**; 264:1941–4.
8. Duraisingh MT, Maier AG, Triglia T, Cowman AF. Erythrocyte- binding antigen 175 mediates invasion in *Plasmodium falciparum* utilizing sialic acid-dependent and independent pathways. Proc Natl Acad Sci U S A **2003**; 100:4796–801.
9. Spadafora C, Awandare GA, Kopydlowski KM, et al. Complement receptor 1 is a sialic acid-independent erythrocyte receptor of *Plasmodium falciparum*. PLoS Pathog **2010**; 6:e1000968.
10. Langermans JA, Hensmann M, van Gijlswiik M, et al. Preclinical evaluation of a chimeric malaria vaccine candidate in Montanide ISA 720: immunogenicity and safety in rhesus macaques. Hum Vaccin **2006**; 2:222–6.
11. Ellis RD, Martin LB, Schaffer D, et al. Phase 1 trial of the *Plasmodium falciparum* blood stage vaccine MSP1 (42)- C1/Alhydrogel with and without CPG 7909 in malaria naïve adults. PLoS One **2010**; 5:e8787.
12. Goel VK, Li X, Chen H, Liu SC, Chishti AH, Oh SS. Band 3 is a host receptor binding merozoite surface protein 1 during the *Plasmodium falciparum* invasion of erythrocytes. Proc Natl Acad Sci U S A **2003**; 100:5164–9.
13. Child MA, Epp C, Bujard H, Blackman MJ. Regulated maturation of malaria merozoite surface protein-1 is essential for parasite growth. Mol Microbiol **2010**; 78:187–202.
14. Holder AA, Blackman MJ, Burghaus PA, et al. A malaria merozoite surface protein (MSP1)-structure, processing and function. Mem Inst Oswaldo Cruz **1992**; 87(suppl 3):37–42.
15. Chappel JA, Holder AA. Monoclonal antibodies that inhibit *Plasmodium falciparum* invasion in vitro recognise the first growth factor-like domain of merozoite surface protein-1. Mol Biochem Parasitol **1993**; 60:303–11.
16. Moss DK, Remarque EJ, Faber BW, et al. *Plasmodium falciparum* 19-kilodalton merozoite surface protein 1 (MSP1)-specific antibodies that interfere with parasite growth in vitro can inhibit MSP1 processing, merozoite invasion, and intracellular parasite development. Infect Immun **2012**; 80:1280–7.
17. Dluzewski AR, Ling IT, Hopkins JM, et al. Formation of the food vacuole in *Plasmodium falciparum*: a potential role for the 19 kDa fragment of merozoite surface protein 1 (MSP1(19)). PLoS One **2008**; 3:e3085.
18. Xiao L, Yang C, Patterson PS, Udhayakumar V, Lal AA. Sulfated polyanions inhibit invasion of erythrocytes by plasmodial merozoites and cytoadherence of endothelial cells to parasitized erythrocytes. Infect Immun **1996**; 64:1373–8.
19. Kisilevsky R, Crandall I, Szarek WA, et al. Short-chain aliphatic polysulfonates inhibit the entry of *Plasmodium* into red blood cells. Antimicrob Agents Chemother **2002**; 46:2619–26.
20. Adams Y, Freeman C, Schwartz-Albiez R, Ferro V, Parish CR, Andrews KT. Inhibition of *Plasmodium falciparum* growth in vitro and adhesion to chondroitin-4-sulfate by the heparan sulfate mimetic PI-88 and other sulfated oligosaccharides. Antimicrob Agents Chemother **2006**; 50:2850–2.
21. Dalton JP, Hudson D, Adams JH, Miller LH. Blocking of the receptor-mediated invasion of erythrocytes by *Plasmodium knowlesi* malaria with sulfated polysaccharides and glycosaminoglycans. Eur J Biochem **1991**; 195:789–94.
22. Basseri HR, Doosti S, Akbarzadeh K, Nateghpour M, Whitten MM, Ladoni H. Competency of *Anopheles stephensimysorensis* strain for *Plasmodium vivax* and the role of inhibitory carbohydrates to block its sporogenic cycle. Malar J **2008**; 7:131.
23. Boyle MJ, Richards JS, Gilson PR, Chai W, Beeson JG. Interactions with heparin-like molecules during erythrocyte invasion by *Plasmodium falciparum* merozoites. Blood **2010**; 115:4559–68.
24. O'Donnell RA, de Koning-Ward TF, Burt RA, et al. Antibodies against merozoite surface protein (MSP)-1(19) are a major component of the invasion-inhibitory response in individuals immune to malaria. J Exp Med **2001**; 193:1403–12.
25. Wu G, Robertson DH, Brooks CL III, Vieth M. Detailed analysis of grid-based molecular docking: a case study of CDOCKER- A CHARMm-based MD docking algorithm. J Comput Chem **2003**; 24:1549–62.
26. Venkatachalam CM, Jiang X, Oldfield T, Waldman M. LigandFit: a novel method for the shape-directed rapid docking of ligands to protein active sites. J Mol Graph Model **2003**; 21:289–307.
27. Shoichet BK. Virtual screening of chemical libraries. Nature **2004**; 432:862–5.
28. Gaonkar SL, Lokanatha Rai KM, Suchetha Shetty N. Microwave-assisted synthesis and evaluation of anti- inflammatory activity of new series of N- substituted 2-butyl-5- chloro- 3 H-imidazole- 4- carbaldehyde derivatives. Med Chem Res **2009**; 18:221–30.
29. Morgan WD, Birdsall B, Frenkiel TA, et al. Solution structure of an EGF module pair from the *Plasmodium falciparum* merozoite surface protein 1. J Mol Biol **1999**; 289:113–22.
30. Babon JJ, Morgan WD, Kelly G, Eccleston JF, Feeney J, Holder AA. Structural studies on *Plasmodium vivax* merozoite surface protein-1. Mol Biochem Parasitol **2007**; 153:31–40.
31. Garman SC, Simcoke WN, Stowers AW, Garboczi DN. Structure of the C-terminal domains of merozoite surface protein-1 from *Plasmodium knowlesi* reveals a novel histidine binding site. J Biol Chem **2003**; 278:7264–9.
32. Johnsson B, Löfås S, Lindquist G. Immobilization of proteins to a carboxymethyldextran-modified gold surface for biospecific interaction analysis in surface plasmon resonance sensors. Anal Biochem **1991**; 198:268–77.
33. Myszka DG. Improving biosensor analysis. J Mol Recognit **1999**; 12: 279–84.
34. Wei L, Jiang P, Yau YH, et al. Residual structure in islet amyloid polypeptide mediates its interactions with soluble insulin. Biochemistry **2009**; 48:2368–76.

35. Sriprawat K, Kaewpongsri S, Suwanarusk R, et al. Effective and cheap removal of leukocytes and platelets from *Plasmodium vivax* infected blood. Malar J **2009**; 8:115.
36. Russell B, Suwanarusk R, Borlon C, et al. A reliable *ex vivo* invasion assay of human reticulocytes by *Plasmodium vivax*. Blood **2011**; 118: e74–81.
37. Malleret B, Claser C, Ong AS, et al. A rapid and robust tri-color flow cytometry assay for monitoring malaria parasite development. Sci Rep **2011**; 1:118.
38. Ishida K, Wierzba MK, Teruya T, Simizu S, Osada H. Novel heparan-sulfate mimetic compounds as antitumor agents. Chem Biol **2004**; 11:367–77.
39. Basappa , Murugan S, Kavitha CV, et al. A small oxazine compound as an anti-tumor agent: a novel pyranoside mimetic that binds to VEGF, HB- EGF, and TNF-α. Cancer Lett **2010**; 297:231–43.
40. Basappa , Sugahara K, Thimmaiah KN, Bid HK, Houghton PJ, Rangappa KS. Anti-tumor activity of a novel HS-mimetic vascular endothelial growth factor binding small molecule. PLoS ONE **2012**; 7:e39444. doi:10.1371/journal.pone.0039444.
41. Wilson DW, Crabb BS, Beeson JG. Development of fluorescent *Plasmodium falciparum* for *in vitro* growth inhibition assays. Malar J **2010**; 9:152.
42. Chandramohanadas R, Davis PH, Beiting DP, et al. Apicomplexan parasites co-opt host calpains to facilitate their escape from infected cells. Science **2009**; 324:794–7.
43. Treeck M, Zacherl S, Herrmann S, et al. Functional analysis of the leading malaria vaccine candidate AMA- 1 reveals an essential role for the cytoplasmic domain in the invasion process. PLoS Pathog **2009**; 5: e1000322.
44. Boyle MJ, Wilson DW, Richards JS, et al. Isolation of viable *Plasmodium falciparum* merozoites to define erythrocyte invasion events and advance vaccine and drug development. Proc Natl Acad Sci U S A **2010**; 107:14378–83.
45. Han HJ, Park SG, Kim SH, et al. Epidermal growth factor-like motifs 1 and 2 of *Plasmodium vivax* merozoite surface protein 1 are critical domains in erythrocyte invasion. Biochem Biophys Res Commun **2004**; 320:563–70.
46. Iyer J, Grüner AC, Rénia L, Snounou G, Preiser PR. Invasion of host cells by malaria parasites: a tale of two protein families. Mol Microbiol **2007**; 65:231–49.
47. Greenbaum DC, Baruch A, Grainger M, et al. A role for the protease falcipain 1 in host cell invasion by the human malaria parasite. Science **2002**; 298:2002–6.
48. Koussis K, Withers-Martinez C, Yeoh S, et al. A multifunctional serine protease primes the malaria parasite for red blood cell invasion. EMBO J **2009**; 28:725–35.
49. Singh S, Alam MM, Pal-Bhowmick I, Brzostowski JA, Chitnis CE. Distinct external signals trigger sequential release of apical organelles during erythrocyte invasion by malaria parasites. PLoS Pathog **2010**; 6: e1000746.